European Journal of Control (1995) 1:77–96

European Journal of Control

A Flexible Transmission System as a Benchmark for Robust Digital Control*

I. D. Landau, D. Rey, A. Karimi, A. Voda and A. Franco

Laboratoire d'Automatique de Grenoble (INPG/CNRS) and Groupement de Recherche Automatique (CNRS) Ecole Nationale Supérieure d'Ingénieurs Electriciens de Grenoble Domaine Universitaire, Grenoble, France

A benchmark problem for digital robust control design is described. The robustness in stability and in performance of eight solutions to this benchmark which have been presented at the 1995 European Control Conference in Rome (Italy) are evaluated. The eight controllers have been designed using several different methods, including discrete time H_∞ optimisation, quantitative feedback theory, non-integer order control, generalised predictive control, combined pole placement/sensitivity function shaping and model free optimisation. Simulations and experimental results are given.

Keywords: Digital control; Robust control; System identification; Flexible systems

1. Introduction

A flexible transmission system built at the Grenoble Automatic Control Laboratory is considered as a benchmark for robust digital control. This system is characterised by two vibration modes with very low damping factors (less than 0.05). The frequencies of these vibration modes change significantly with load, while the damping factors still remain very low. Adaptive control [1,2] has been considered as an issue for this control problem.

The discrete time identified models of the system for the extreme situations (no load and full load) as well as for an intermediate situation are given. The objective is to design a robust digital controller to maintain satisfactory stability and performance characteristics for the three models.

This paper is organised as follows: Section 2 presents the flexible transmission system. The benchmark specifications are described in Section 3. The characteristics of different controllers are demonstrated in Section 4. In Section 5 the simulation results obtained by various controllers are evaluated. Section 6 gives the experimental results.

2. The Flexible Transmission

The flexible transmission consists of three horizontal pulleys connected by two elastic belts (Fig. 1). The

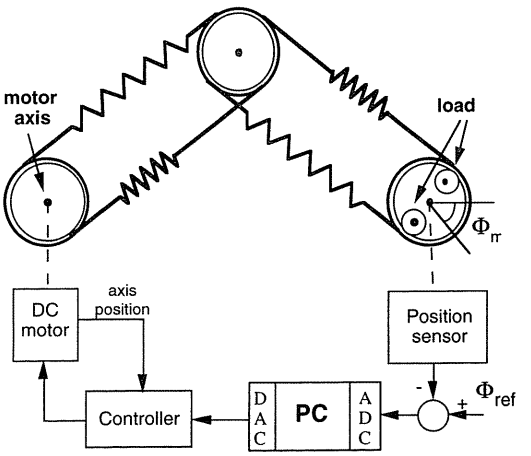

Fig. 1. Schematic diagram of the flexible transmission.

* Work supported by G.R. Automatique (CNRS).

Paper presented at ECC 95, Rome, 5–8 September 1995.

Correspondence to: I. D. Landau, Laboratoire d'Automatique de Grenoble Domaine Universitaire, 38402 Saint-Martin d'Hères, France. E-mail: landau@lag.grenet.fr

Received 15 May 1995; Accepted in revised form 28 July 1995
Recommended by S. Graebe and D. Clarke

first pulley is driven by a DC motor whose position is controlled by local feedback. The third pulley may be loaded with small disks of different weight. The system input is the reference for the axis position of the first pulley. The system output is the axis position of the third pulley measured by a position sensor, sampled and digitised. A PC is used to control the system.

The low damped vibration modes, the large variations of their frequencies with the load and the availability of the various identified discrete time models make this experimental device a suitable benchmark for the design of a robust digital controller. The discrete time models of the system (sampling frequency: 20 Hz) for the no load, half load (1.8 kg) and full load (3.6 kg) cases have been identified with a low magnitude PRBS input (using PIM/TR software [3]). For this purpose 256 samples were generated by an 8-bit shift register. Several identification methods have been examined. The *output error with extended prediction model* method [4] gave the best results in all cases. The whiteness test on the residuals was used as the validation test.

The following transfer function is considered as the plant model:

$$H(q^{-1}) = \frac{q^{-d}B(q^{-1})}{A(q^{-1})}$$

where q^{-1} is the backward shift operator $(y(t-1) = q^{-1}y(t))$, d is the integer number of sampling periods contained in the plant pure time delay and:

$$A(q^{-1}) = 1 + a_1q^{-1} + \ldots a_{n_A}q^{-n_A}$$
$$B(q^{-1}) = b_1q^{-1} + b_2q^{-2} + \ldots b_{n_B}q^{-n_B}$$

The corresponding identified and validated models are:

Unloaded model:

$$A(q^{-1}) = 1 - 1.41833q^{-1} + 1.58939q^{-2} - 1.31608q^{-3} + 0.88642q^{-4}$$
$$B(q^{-1}) = 0.28261q^{-1} + 0.50666q^{-2}$$
$$d = 2$$

Half load model:

$$A(q^{-1}) = 1 - 1.99185q^{-1} + 2.20265q^{-2} - 1.84083q^{-3} + 0.89413q^{-4}$$
$$B(q^{-1}) = 0.10276q^{-1} + 0.18123q^{-2}$$
$$d = 2$$

Full load model:

$$A(q^{-1}) = 1 - 2.09679q^{-1} + 2.31962q^{-2} - 1.93353q^{-3} + 0.87129q^{-4}$$
$$B(q^{-1}) = 0.06408q^{-1} + 0.10407q^{-2}$$
$$d = 2$$

The frequency characteristics of the three models are represented in Fig. 2. The strong influence of the load upon the location of the vibration modes is observed. The pole-zero chart of the unloaded model is given in Fig. 3. The damping factors of the vibration modes are less than 0.05 and the model has an unstable zero in addition to a delay $d = 2$.

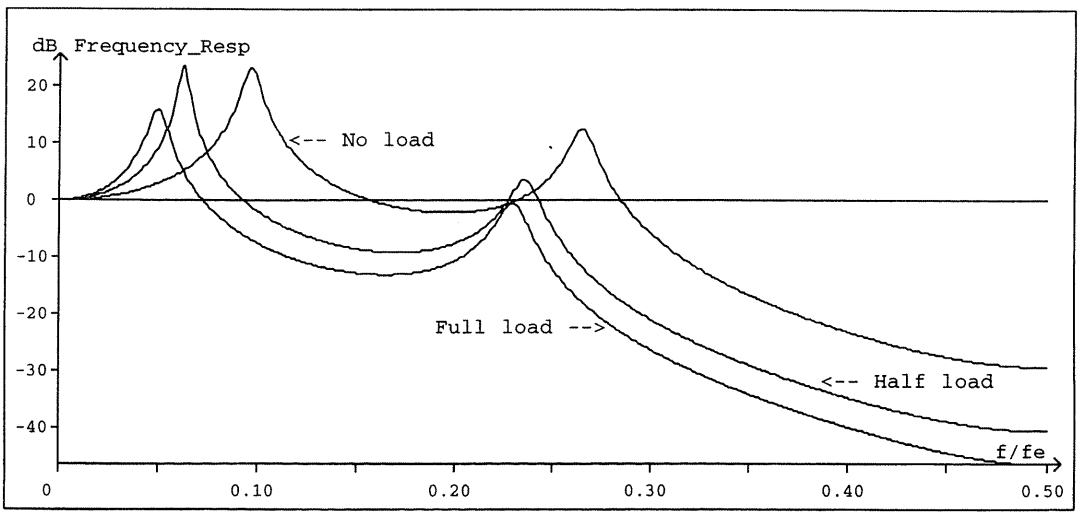

Fig. 2. Frequency characteristics of identified models.

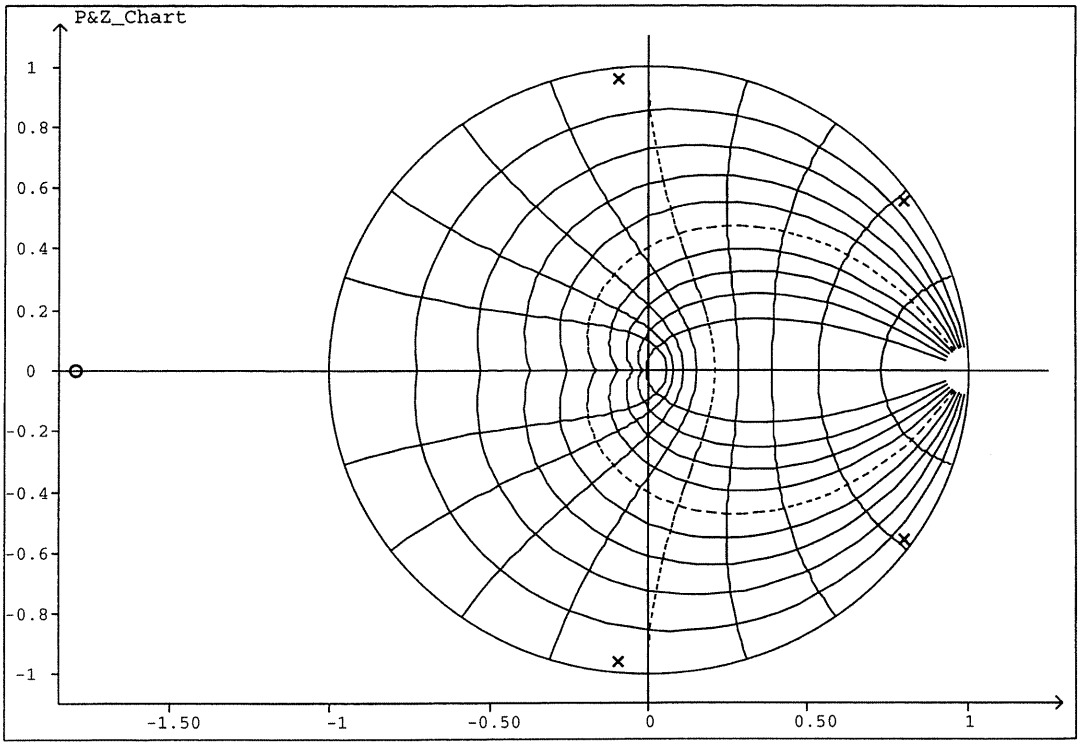

Fig. 3. Pole-zero chart for the unloaded model.

3. Description of the Specifications

A discrete-time two-degree of freedom polynomial form RST controller is to be designed. Figure 4 shows the block diagram of the system with a RST controller (for more details see [4]). This type of controller implemented in polynomial form with a limited precision has been chosen voluntarily in order to check the robustness of the solutions with respect to numerical problems.

The canonical form of the RST controller is given by:

$$S(q^{-1})u(t) = T(q^{-1})y^*(t+d+1) - R(q^{-1})y(t)$$

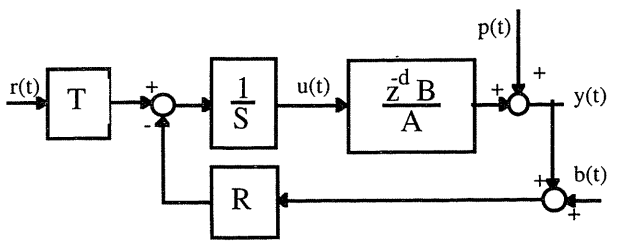

Fig. 4. Closed loop system with a RST controller in presence of output disturbances and measurement noise.

where $u(t)$ is the plant input, $y(t)$ is the plant output, $y^*(t+d+1)$ is the desired tracking (reference) trajectory and R, S, T are polynomials in q^{-1}.

$$R(q^{-1}) = r_0 + r_1 q^{-1} + \ldots + r_{n_R} q^{-n_R}$$
$$S(q^{-1}) = 1 + s_1 q^{-1} + \ldots + s_{n_S} q^{-n_S}$$
$$T(q^{-1}) = t_0 + t_1 q^{-1} + \ldots + t_{n_T} q^{-n_T}$$

The parameters of a RST type controller with a precision of six digits should be computed in order to achieve the following specifications:

(a) A rise time (0–90% of the final value) of less than 1 s for a step change in the reference input for all loads.

(b) Overshoot less than 10% for a step change in the reference input for all loads.

(c) Rejection of step output disturbances filtered by $1/A$ within 1.2 s (for 90% rejection of the measured peak value) for all loads.

(d) Perfect rejection of constant disturbances (using integral action).

(e) Disturbance attenuation in the low frequency band from 0 to 0.2 Hz for all loads.

(f) A maximum value of less than 6 dB of the output sensitivity function (modulus margin greater than 0.5) for all loads.

Remark: The output sensitivity function is the transfer function between the disturbance $p(t)$ and the plant output $y(t)$ (Fig. 4).

$$S_{yp}(z^{-1}) = \frac{A(z^{-1})S(z^{-1})}{A(z^{-1})S(z^{-1}) + z^{-d}B(z^{-1})R(z^{-1})} = \frac{A(z^{-1})S(z^{-1})}{P(z^{-1})}$$

The modulus margin is defined as the radius of the circle centred in [−1, j0] and tangent to the Nyquist plot of the open loop transfer function of the system. It can be shown that the modulus margin is equal to the inverse of the maximum modulus of the output sensitivity function (it is a more significant robustness indicator than gain and phase margin).

(g) A delay margin of at least 40 ms (80% of sampling period).

Remark: The delay margin is the additional delay which will make the system unstable. It can be computed using the phase margin as follows:

$$\Delta\tau = \frac{\Delta\phi}{\omega_{\text{cr}}}$$

Where $\Delta\tau$, $\Delta\phi$ and ω_{cr} are respectively, the delay margin, the phase margin and the crossover frequency. If the Nyquist plot intersects the unit circle at several frequencies ω_{cr}^{i}, characterised by the corresponding phase margin $\Delta\phi_i$, the delay margin is defined by:

$$\Delta\tau = \min_i \frac{\Delta\phi_i}{\omega_{cr}^{i}}$$

(h) A maximum value of less than 10 dB of the input sensitivity function in the frequency range 8–10 Hz for all loads.

Remark: The input sensitivity function is the transfer function between $p(t)$ and the plant input $u(t)$ (Fig. 4)

$$S_{\text{up}}(z^{-1}) = \frac{-A(z^{-1})R(z^{-1})}{A(z^{-1})S(z^{-1}) + z^{-d}B(z^{-1})R(z^{-1})} = \frac{-A(z^{-1})R(z^{-1})}{P(z^{-1})}$$

In the absence of this constraint important excitations of the input occur in a zone where the system gain is very low.

4. Simulation Results

The simulation results of eight solutions to the benchmark problem (which have also been used in the real time experiments) are presented in this section. The eight controllers range from 4th order to 12th order and have been designed using different methods. The designs are as follows (each controller is named by the first letter of the name of the first author):

- Controller D is designed using the constrained receding horizon predictive control (CRHPC) by Decker et al. [5].
- Controller H is designed using a model free scheme by Hjalmarsson et al. [6].
- Controllers J and W are designed using Discrete time H_∞ optimisation method by Jones and Limebeer [7] and Walker [8], respectively. The two designs are based on a discrete time version of McFarlane–Glovers normalised coprime factorisation method. In the paper by Walker a simple shaping filter is used in order to obtain a low order controller and this results in failing to meet some of the specifications, whereas Jones and Limebeer use a two degree of freedom controller with two more complex shaping filters which consequently results in a high order controller satisfying almost all of the specifications.
- Controllers K and N are designed using quantitative feedback theory (QFT) by Kidron and Yaniv [9] and Nordin and Gutman [10], respectively. While the paper of Nordin and Gutman seems to be a straightforward application of the QFT method (via a prewarped bilinear transformation), Kidron and Yaniv use in their design some new results for approximating the closed loop behaviour around the resonance frequencies (both for the continuous and discrete time cases).
- Controller L is designed using combined pole placement/sensitivity function shaping method by Landau et al. [11].
- Controller O is designed using the non-integer order type control by Oustaloup et al. [12].

It should be noticed that in the designs of H, K, L, N and O the information provided on the model uncertainty has been taken into account while the designs J and W try to maximise the robustness without considering the information on model uncertainty. The controller D has been obtained as the result of a trial and error design.

All of the designs except for N and O are based on a direct discrete time approach. The controllers N and O have been computed in the continuous time domain and have been transferred to the discrete time domain via a prewarped bilinear transformation.

The characteristics of different designs have been recomputed using the PC-REG software [3] for comparison purposes and are presented in the following tables and histograms.

4.1. Rise Time

In the three different loadings, designs J, K and N satisfy this specification and designs L and H almost meet it. The fastest controller is N and the slowest one is W (for the unloaded case). Table 1 and Fig. 5 show the rise time (s) of various designs for no load, half load and full load cases.

Table 1. The rise time (s) for various designs.

	No load	Half load	Full load
D	1.342	1.315	0.864
H	1.089	1.017	0.911
J	0.949	0.801	0.836
K	0.995	0.922	0.839
L	1.056	0.900	0.934
N	0.813	0.598	0.660
O	1.168	1.114	0.973
W	2.325	2.230	1.960

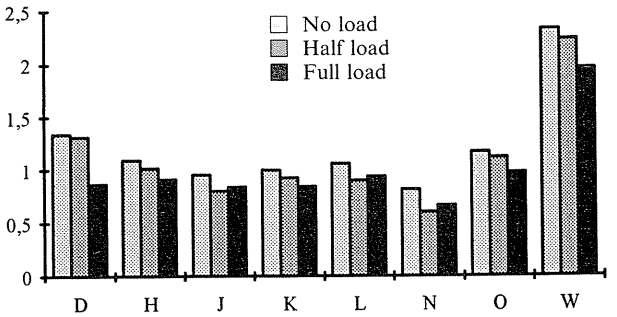

Fig. 5. The histogram of rise time (s) for various designs.

4.2. Overshoot

Almost all of the designs satisfy the condition on the overshoot; O, D, W and H have the minimum overshoot. Maximum overshoot occurs for the full load case in all of the designs except for W. Table 2 and Fig. 6 show the overshoot (%) of various designs.

Table 2. The overshoot (%) for various designs.

	No load	Half load	Full load
D	0%	0%	0.81%
H	0.25%	0.04%	0.91%
J	1.50%	2.45%	10.35%
K	5.16%	6.15%	4.49%
L	0%	0.59%	10.02%
N	0.26%	0.89%	9.27%
O	0.01%	0.05%	0.08%
W	0%	0.67%	0.04%

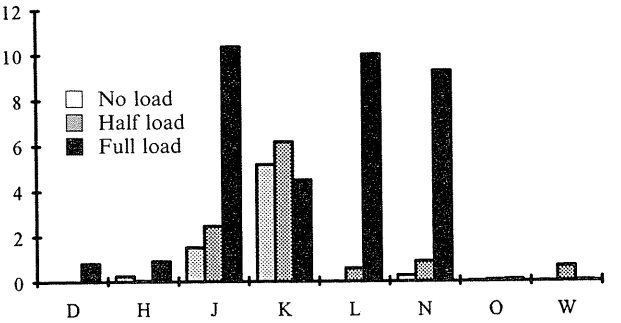

Fig. 6. The histogram of overshoot (%) for various designs.

4.3. Disturbance Rejection

This specification is achieved by controllers K, N and O and it is almost satisfied by L, H and J. Design W is very far from the specification. Table 3 and Fig. 7 illustrate the disturbance rejection time (s) of various designs.

Table 3. The disturbances rejection time (s) for various designs.

	No load	Half load	Full load
D	1.468	1.383	1.842
H	1.069	0.728	1.300
J	1.251	1.275	0.910
K	1.095	1.189	0.908
L	1.114	1.244	0.889
N	1.115	1.152	1.153
O	1.113	1.198	1.123
W	1.783	2.976	3.257

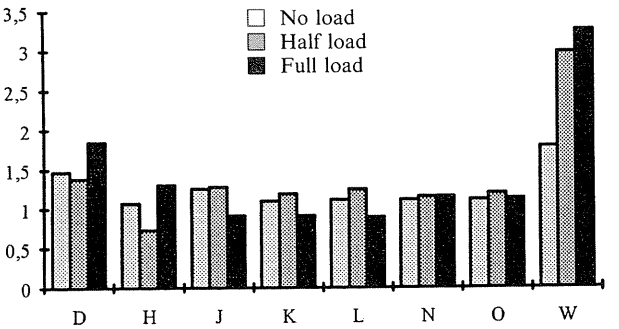

Fig. 7. The histogram of disturbances rejection time (s) for various designs.

4.4. Maximum of S_{yp}

This specification is almost met by all of the controllers. Table 4 and Fig. 8 show the maximum of S_{yp} (dB) of various designs.

Table 4. The maximum of Syp (dB) for various designs.

	No load	Half load	Full load
D	6.00	4.17	5.31
H	5.76	5.14	6.11
J	5.45	4.63	5.26
K	5.67	5.06	5.57
L	5.34	5.31	5.99
N	4.92	4.38	5.23
O	4.74	4.35	5.06
W	2.11	4.2	4.91

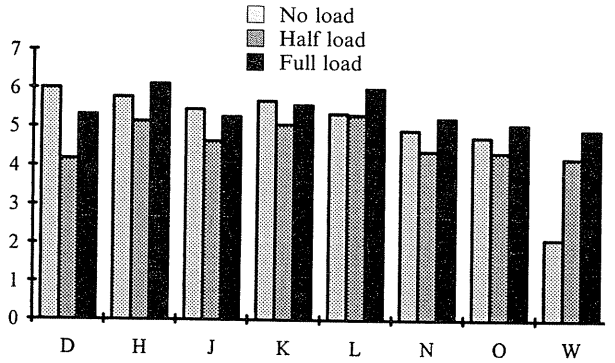

Fig. 8. The histogram of maximum of Syp (dB) for various designs.

4.5. Maximum of S_{up}

This specification is met by all of the controllers. Design W has a value less than 0 dB for all loads. Table 5 and Fig. 9 show the maximum of S_{up} (dB) of various designs in the frequency range 8–10 Hz.

Table 5. The maximum of Sup (dB) for various designs.

	No load	Half load	Full load
D	8.10	8.57	8.69
H	9.84	9.53	9.66
J	6.80	7.62	7.77
K	9.41	9.73	9.87
L	5.90	5.80	5.79
N	9.63	8.74	8.71
O	0.91	0.90	0.91
W	<0	<0	<0

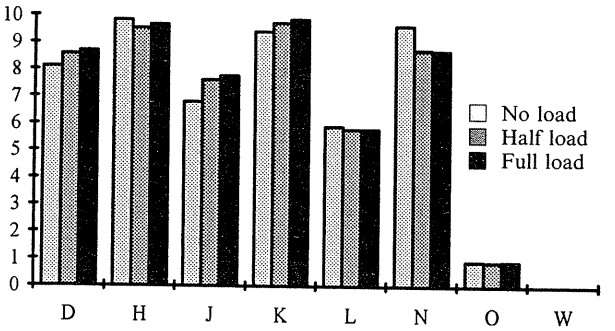

Fig. 9. The histogram of maximum of Sup (dB) for various designs.

4.6. Delay Margin

All of the controllers except for J (for unloaded case) meet this specification. Table 6 and Fig. 10 show the delay margin (ms) of various designs.

Table 6. The delay margin (ms) for various designs.

	No load	Half load	Full load
D	53	221	495
H	54	120	388
J	24	84	412
K	48	102	366
L	43	100	487
N	57	163	410
O	40	106	509
W	140	350	1663

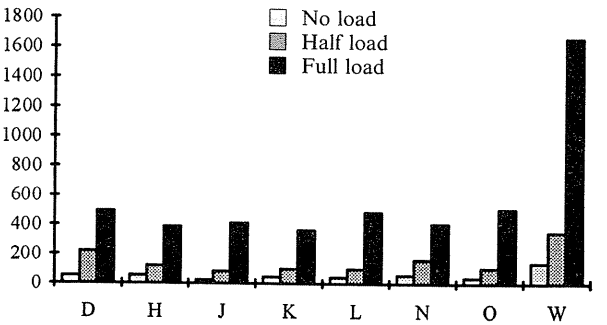

Fig. 10. The histogram of delay margin (ms) for various designs.

4.7. Attenuation Band

This specification is met by controllers N and O. It is almost satisfied by D. The attenuation bands in Hz are shown in Table 7 and Fig. 11.

Table 7. The attenuation band (Hz) for various designs.

	No load	Half load	Full load
D	0.190	0.190	0.190
H	0.180	0.180	0.176
J	0.158	0.160	0.154
K	0.168	0.170	0.186
L	0.164	0.170	0.164
N	0.202	0.204	0.200
O	0.200	0.202	0.198
W	0.178	0.180	0.170

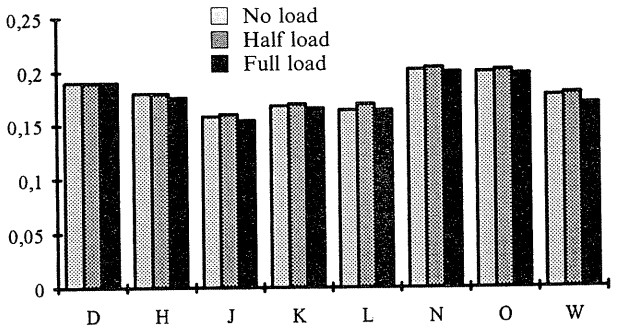

Fig. 11. The histogram of attenuation band (Hz) for various designs.

4.8. Settling Time

There is not any condition on settling time in the benchmark specifications. However, it is very interesting to compare different designs by this characteristic. The settling time is the time required for the step response curve to reach and stay within 2% of the final value. Table 8 and Fig. 12 show the settling time (s) of various designs. The controller W has the maximum and design J has the minimum settling time.

Table 8. The settling time (s) for various designs.

	No load	Half load	Full load
D	2.142	2.280	2.913
H	1.583	1.650	2.100
J	1.273	1.800	2.013
K	2.508	2.384	2.305
L	1.473	2.387	2.281
N	1.667	1.961	1.923
O	1.632	1.510	2.106
W	3.883	3.962	4.914

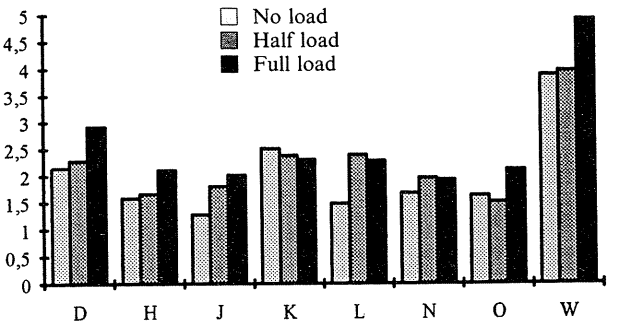

Fig. 12. The histogram of settling time (s) for various designs.

5. Evaluation of the Designs

A performance index for evaluating the different controllers was determined. This performance index may be defined as the average of satisfactory ratios computed for each specification. The satisfactory ratio is 100% if a condition is achieved by a controller and it is 0% if the corresponding characteristic is two times greater (or less) than the limit value. The intermediate values are computed by linear interpolation.

This criterion is equal to 100% for controller N which satisfies all of the specifications in simulation. It is more than 97% for O, K, H and L, and more than 91% for J and D. The controller W has met only about 72% of the specifications. Figure 13 shows the histogram of the performance index in percent in the various designs.

The complexity of the controllers, i.e. the order of R, S and T, may also be considered for evaluating the designs. Table 9 and Fig. 14 demonstrate the complexity of the controllers in terms of the orders of the polynomials R,S and T. The minimum complexity is achieved by the controller H and K. The controller J has the maximum complexity among all of the designs.

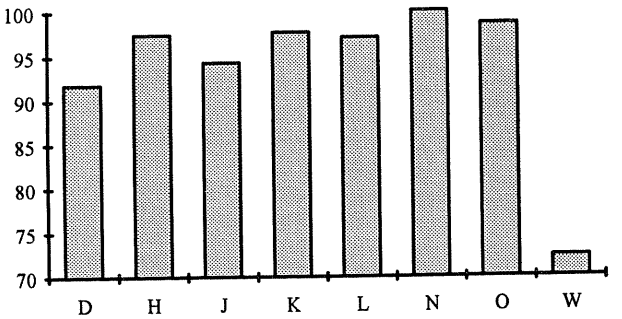

Fig. 13. The histogram of the performance index.

Table 9. The controller order for the various designs.

	R	S	T	sum
D	4	4	8	16
H	4	1	4	9
J	10	12	13	35
K	4	4	1	9
L	6	6	0	12
N	9	9	2	20
O	7	7	0	14
W	5	5	5	15

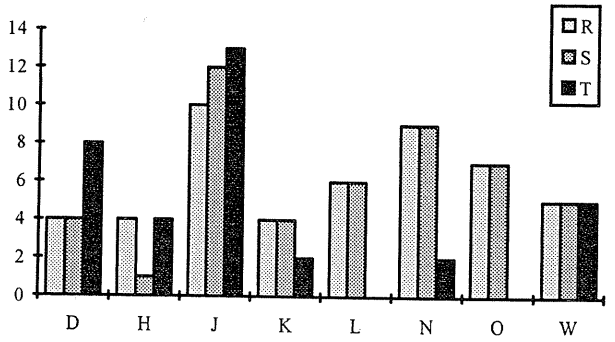

Fig. 14. The histogram of the complexity of the various designs.

Table 10 gives a joint evaluation of the performance and complexity of the various controllers. It is observed that one has to pay the price of the performance by augmenting the complexity.

Table 10. The joint performance/complexity evaluation.

	Performance (%)	Complexity (order of $R+S+T$)
N	100	20
O	98.61	14
K	97.71	9
H	97.48	9
L	97.12	12
J	94.38	35
D	91.82	16
W	72.35	15

6. Experimental Results

The mechanical modifications made to the flexible transmission, presented in the second section, after the benchmark problem had been sent out, caused some changes in the dynamic characteristics of the system. It has become less damped in particular at the full load and therefore more difficult to control. For comparison, the frequency responses of previous models and of the new ones are given in Fig. 15(a,b,c). However, since the designs are robust, we tried to apply the controllers in the modified transmission system. The real time experiments have been carried out using the PCREG-TR real time software [3].

At the time of the first experiments the designs D, H and L were successfully examined on the real system. But we were not able to test the other designs which had a too small static feedback gain (R(1) smaller than 0.01). This problem may occur for controllers with approximate pole-zeros cancellation close to 1 and it may be solved by removing these pole-zeros from the controller. The real time experiments of such controllers were carried out after the controllers had been modified by the authors.

Figures 16–39 illustrate the step and disturbance responses of various designs for different loads. For comparison the step and disturbance responses in simulation are also plotted in the same figures. The models of the modified transmission system have been used in these simulations. It is observed that there are some differences between the simulations and the real time experiments. It may be because the open loop identified models are not the perfect models for controller design. In [13], it is shown that designs based on closed loop identified models give much closer results in simulation and in real time experiments.

The disturbances on the real plant correspond to a slow position displacement followed by a quick release. Therefore the interesting part starts after the response crosses over the steady state value. Since the disturbances are applied manually, we have small changes in the magnitude of the disturbances in different tests. The output disturbances are also simulated and are shown in the same figures. The simulated disturbances are applied before the real ones to better illustrate the curves.

Table 11 and Fig. 40 show the rise times obtained on the real platform. It is observed, generally, that the real system is slower than the simulated one using the open loop identified models. The fastest controller in different loadings is the controller N. The other controllers may be sorted from the fastest to the slowest one as follows: J, K, L, O, H, D and W.

Table 12 shows the settling times obtained on the real platform for different loads. Since the noise to signal ratio is about 3% for the real time applications the settling time is defined as the time required for the step response curve to reach and stay within 5% of the final value. The histogram of the settling time is illustrated in Fig. 41. The minimum settling time for

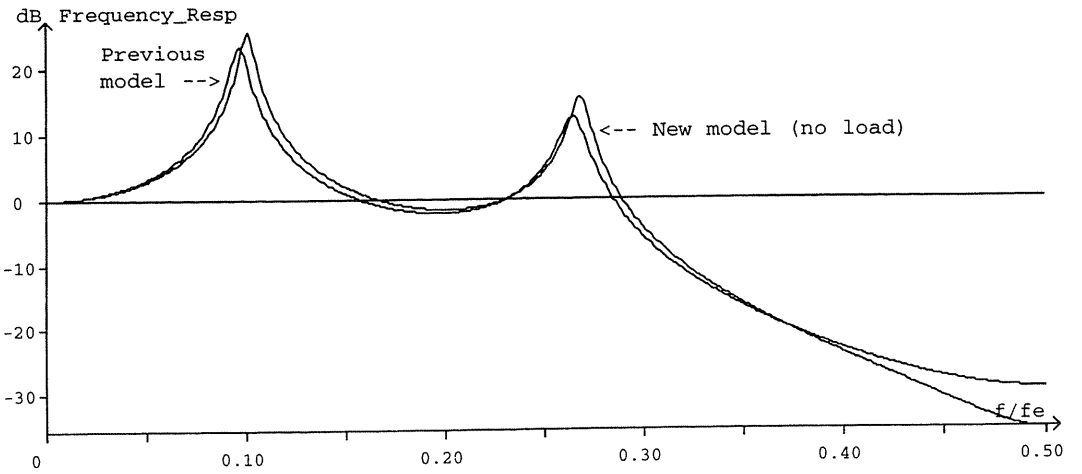

a

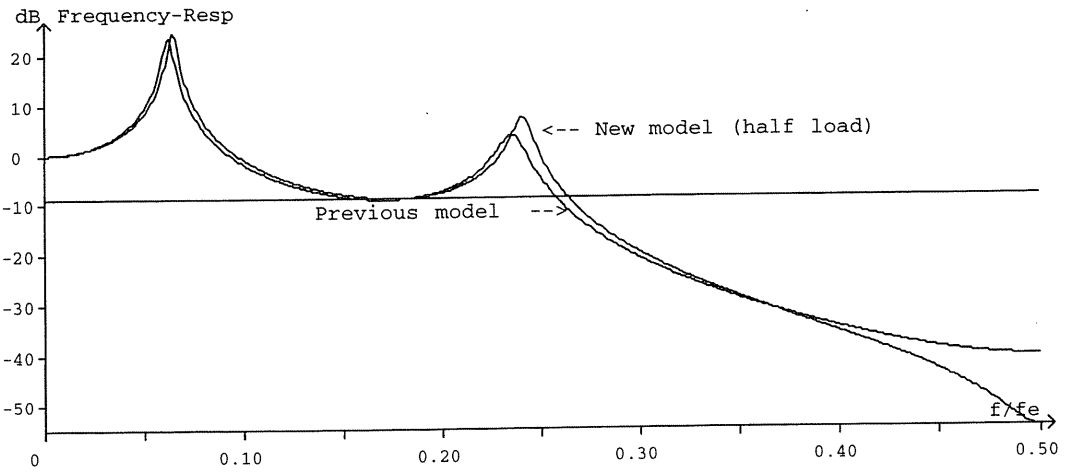

b

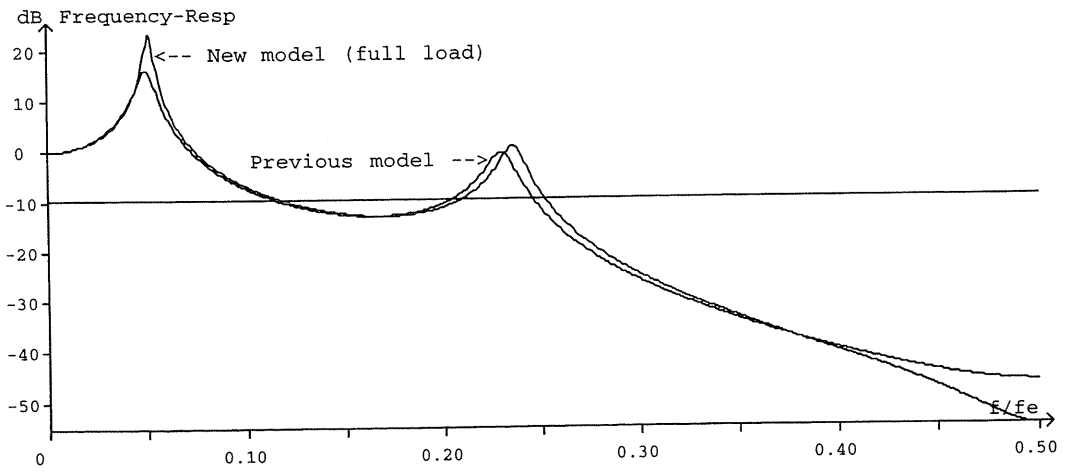

c

Fig. 15. Frequency responses for the new and previous models. **a** no load; **b** half load; **c** full load.

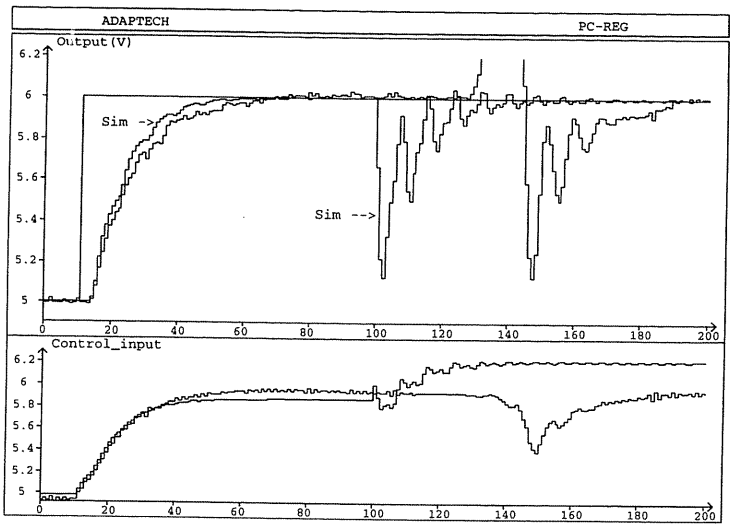

Fig. 16. Step and disturbance responses for unloaded case (Design D).

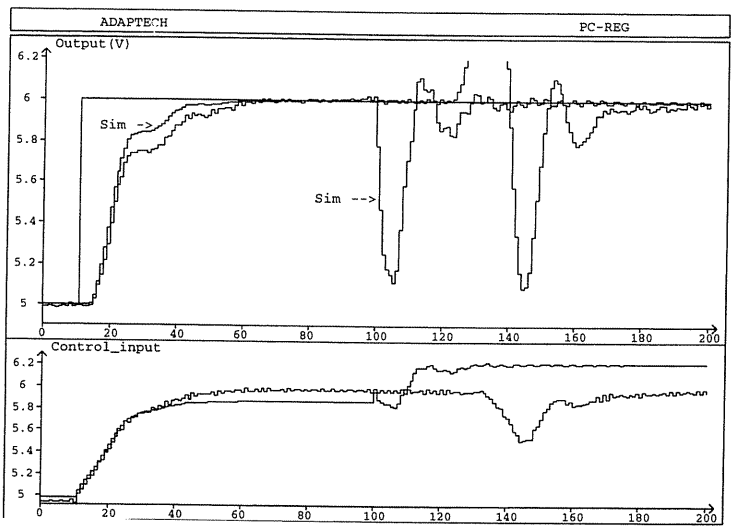

Fig. 17. Step and disturbance responses for half load case (Design D).

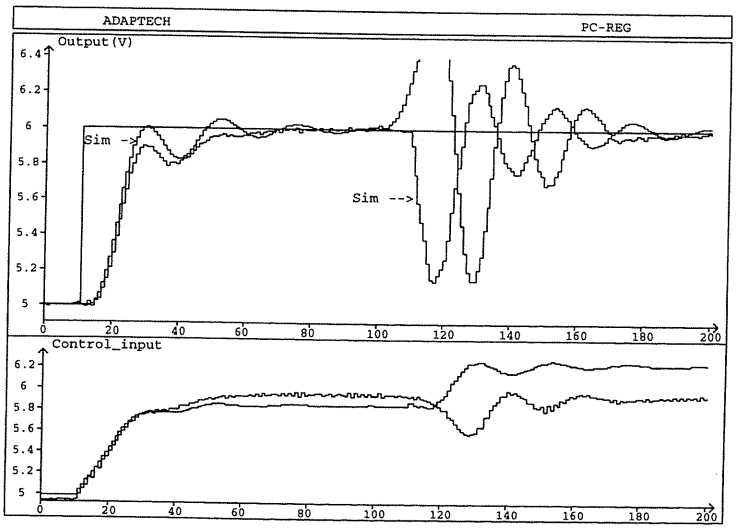

Fig. 18. Step and disturbance responses for full load case (Design D).

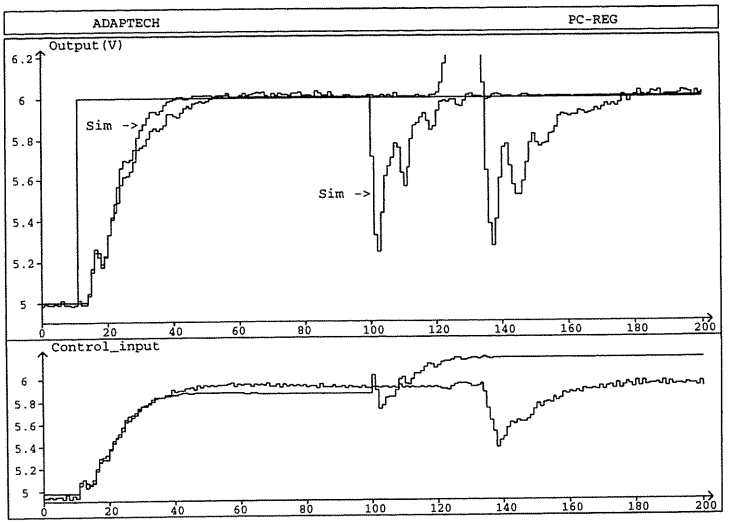

Fig. 19. Step and disturbance responses for unloaded case (Design H).

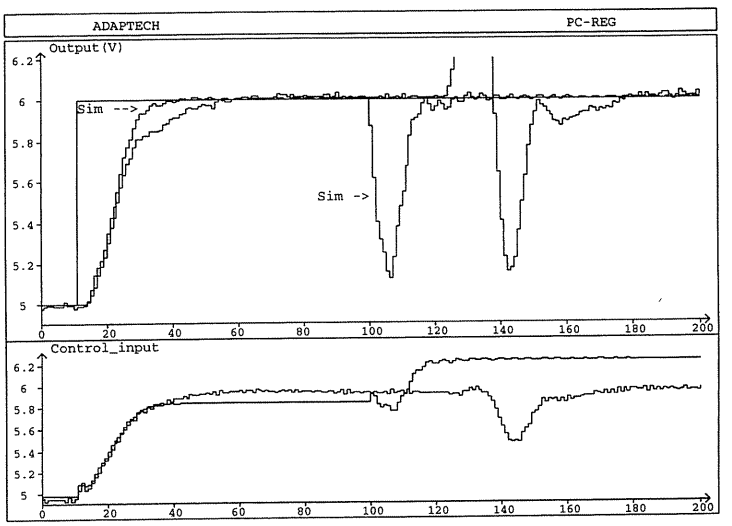

Fig. 20. Step and disturbance responses for half load case (Design H).

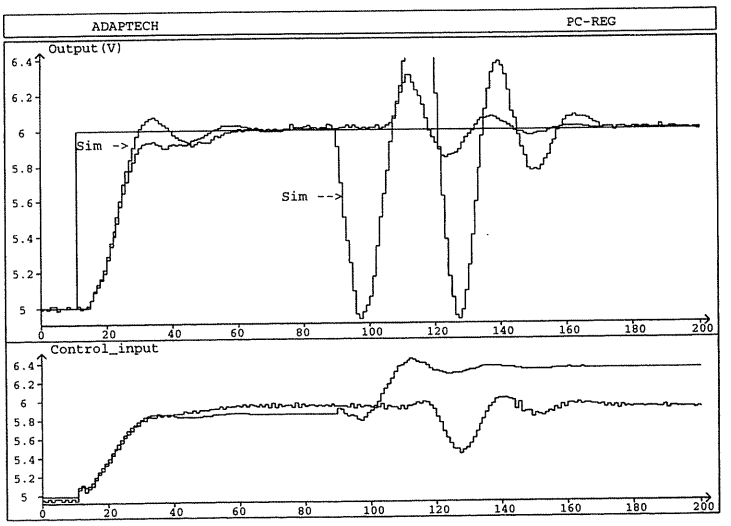

Fig. 21. Step and disturbance responses for full load case (Design H).

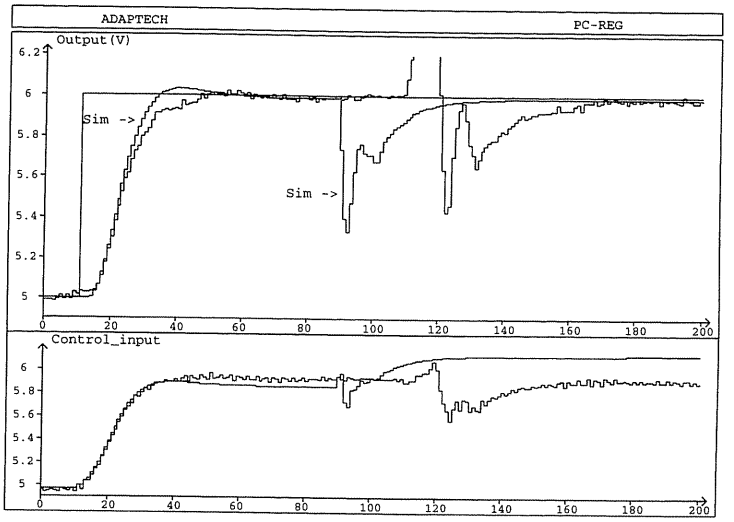

Fig. 22. Step and disturbance responses for unloaded case (Design J).

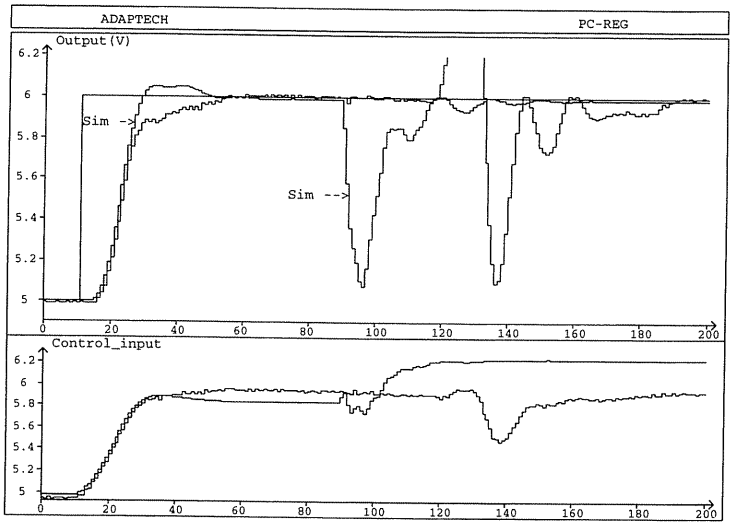

Fig. 23. Step and disturbance responses for half load case (Design J).

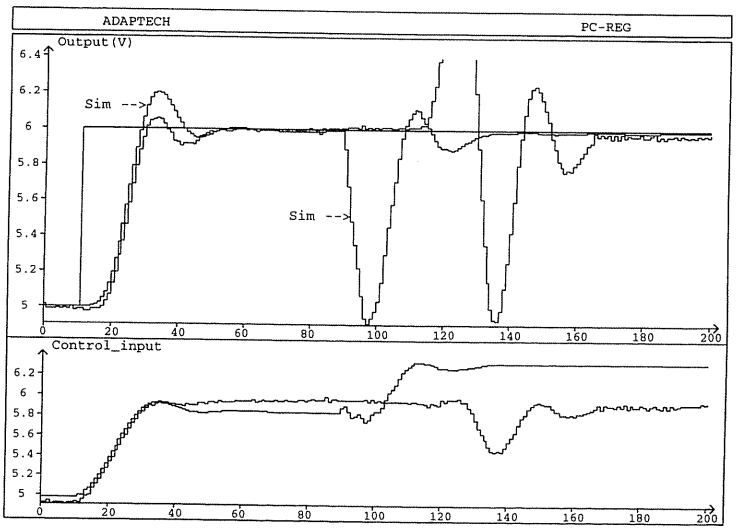

Fig. 24. Step and disturbance responses for full load case (Design J).

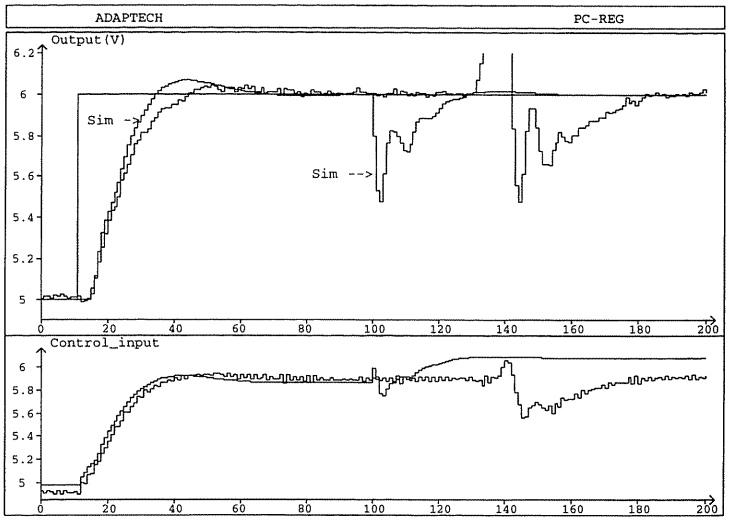

Fig. 25. Step and disturbance responses for unloaded case (Design K).

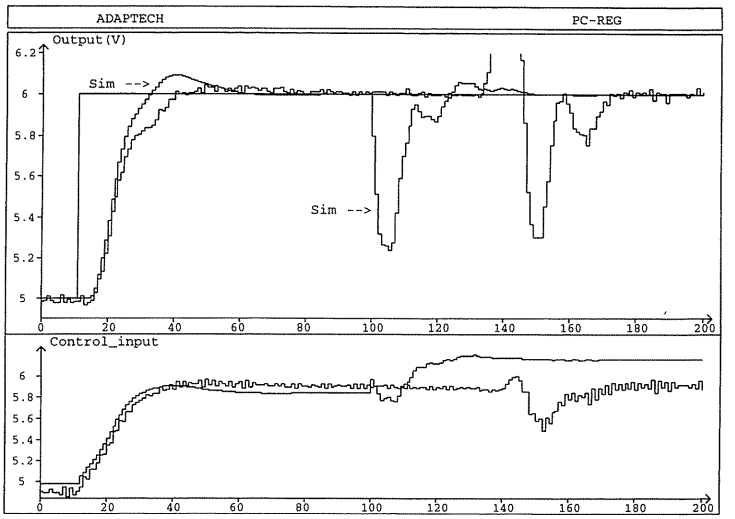

Fig. 26. Step and disturbance responses for half load case (Design K).

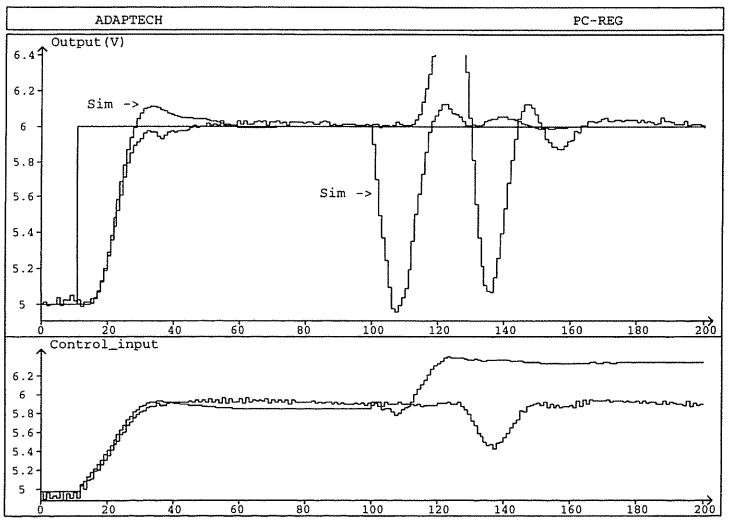

Fig. 27. Step and disturbance responses for full load case (Design K).

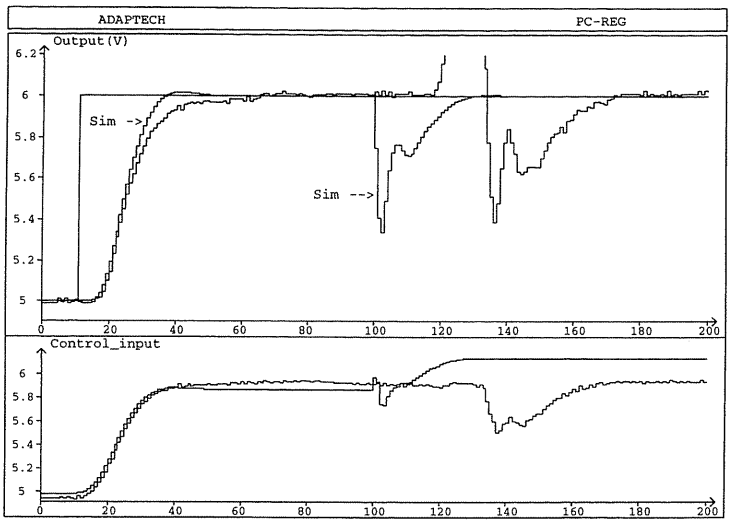

Fig. 28. Step and disturbance responses for unloaded case (Design L).

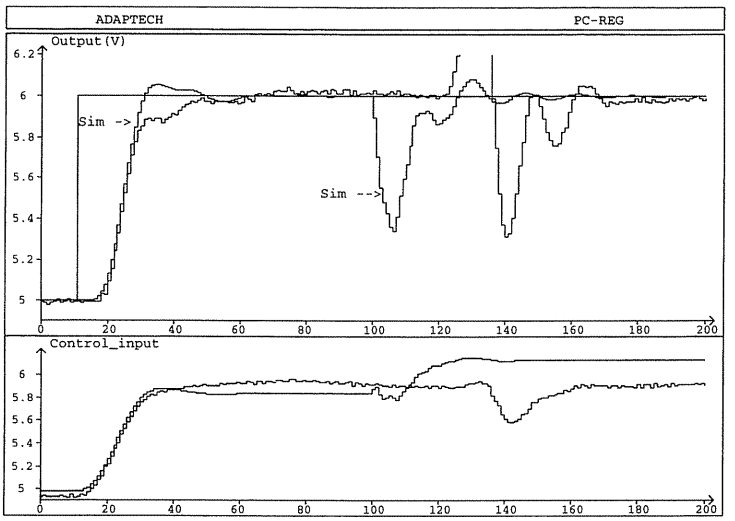

Fig. 29. Step and disturbance responses for half load case (Design L).

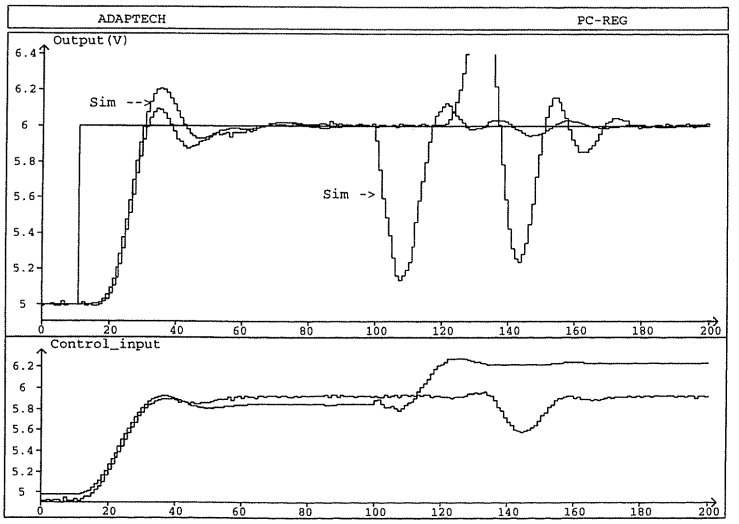

Fig. 30. Step and disturbance responses for full load case (Design L).

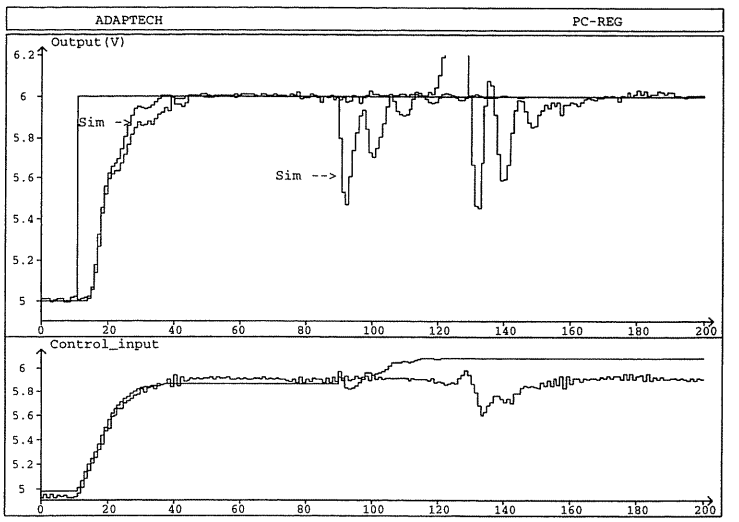

Fig. 31. Step and disturbance responses for unloaded case (Design N).

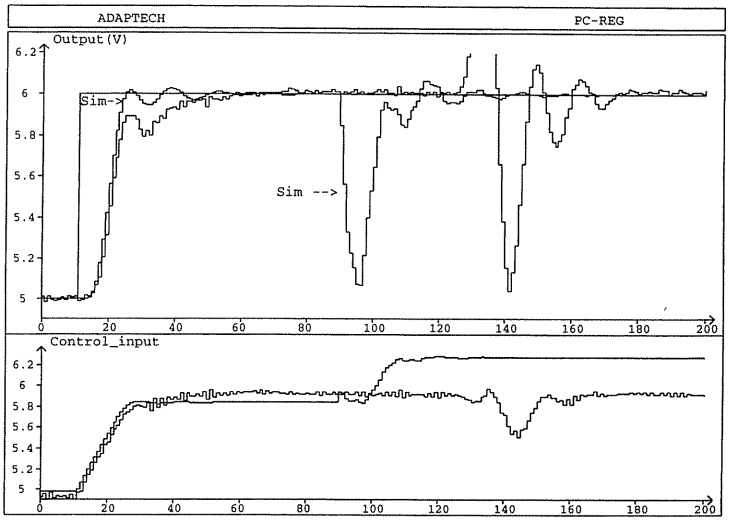

Fig. 32. Step and disturbance responses for half load case (Design N).

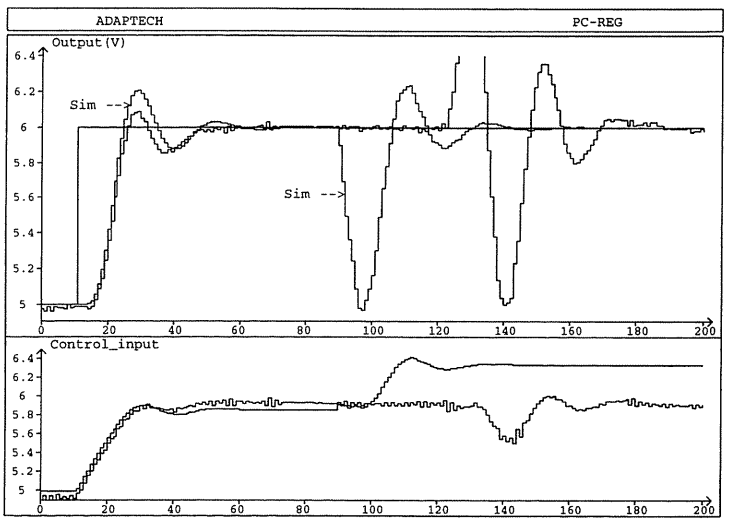

Fig. 33. Step and disturbance responses for full load case (Design N).

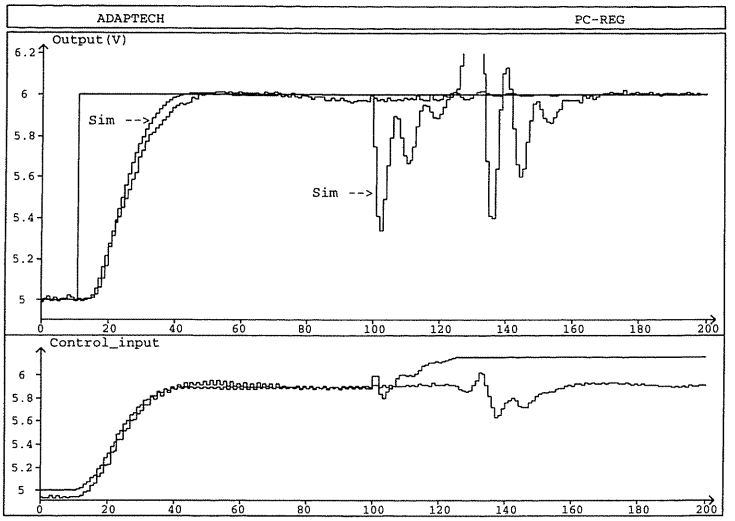

Fig. 34. Step and disturbance responses for unloaded case (Design O).

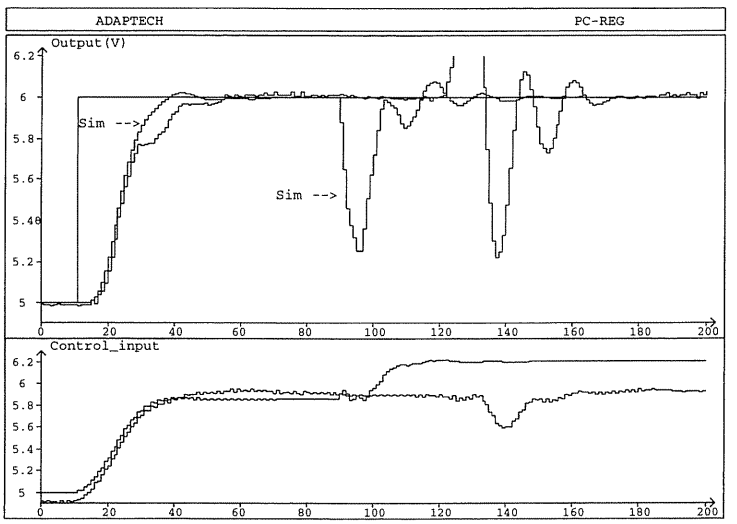

Fig. 35. Step and disturbance responses for half load case (Design O).

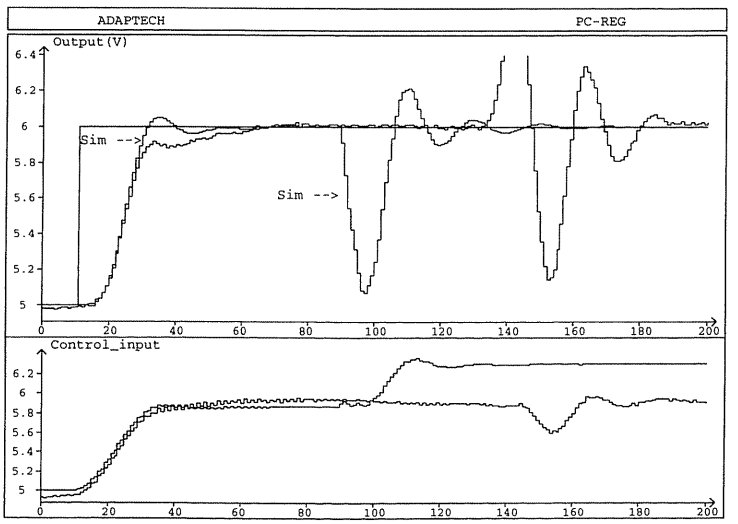

Fig. 36. Step and disturbance responses for full load case (Design O).

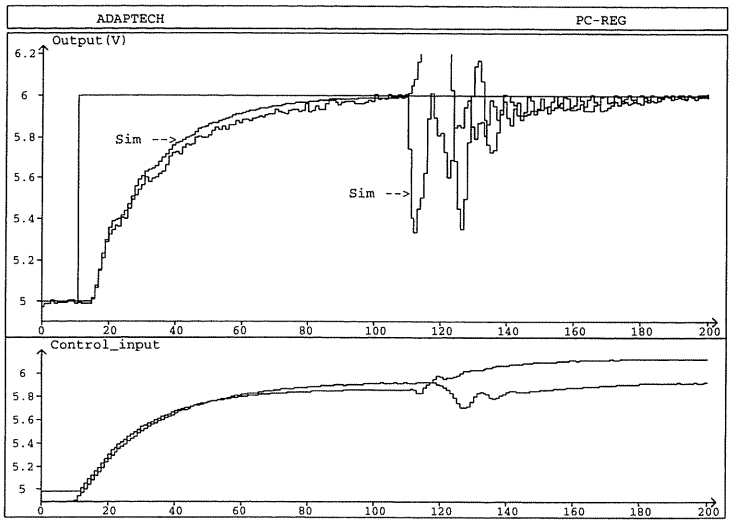

Fig. 37. Step and disturbance responses for unloaded case (Design W).

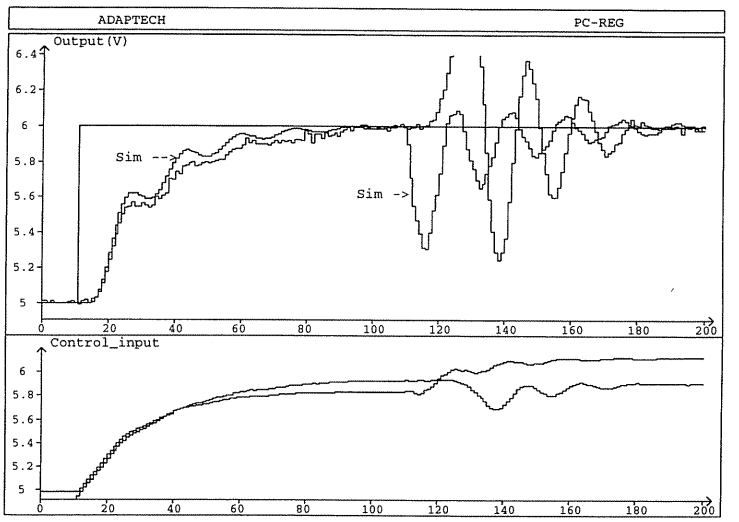

Fig. 38. Step and disturbance responses for half load case (Design W).

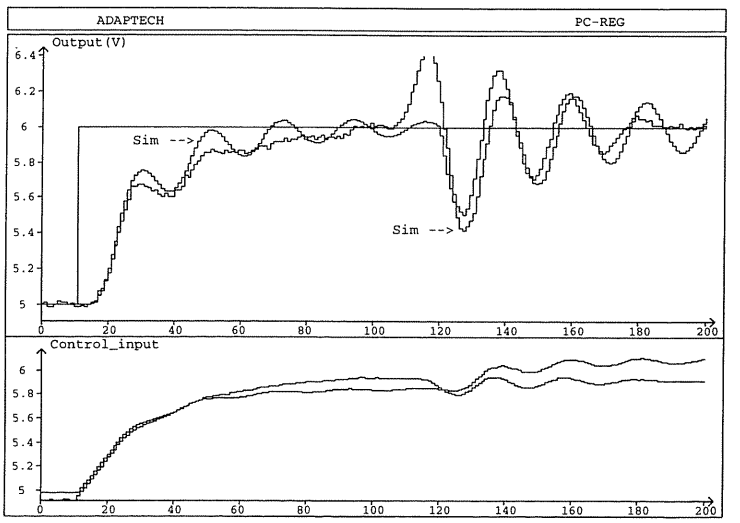

Fig. 39. Step and disturbance responses for full load case (Design W).

Table 11. The rise time (s) in real time application.

	No load	Half load	Full load
D	1.457	1.515	0.887
H	1.334	1.515	0.948
J	1.060	1.245	0.876
K	1.158	1.188	0.842
L	1.255	1.371	0.939
N	1.125	0.697	0.691
O	1.32	1.384	1.090
W	2.804	2.465	2.931

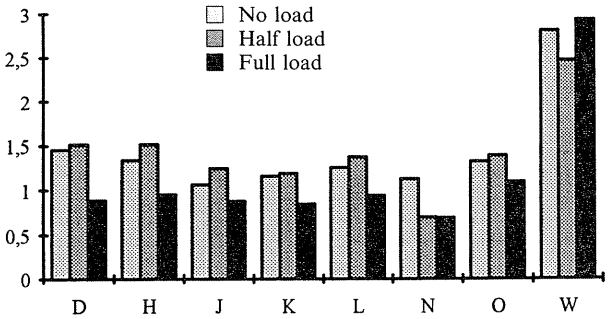

Fig. 40. The histogram of the rise time in real time application.

Table 12. The settling time (s) in real time application.

	No load	Half load	Full load
D	2.15	2.10	2.00
H	1.80	1.70	2.15
J	1.65	1.85	1.80
K	1.45	1.40	1.35
L	1.60	1.65	2.35
N	1.45	2.00	1.80
O	1.55	1.55	2.10
W	3.75	4.00	4.05

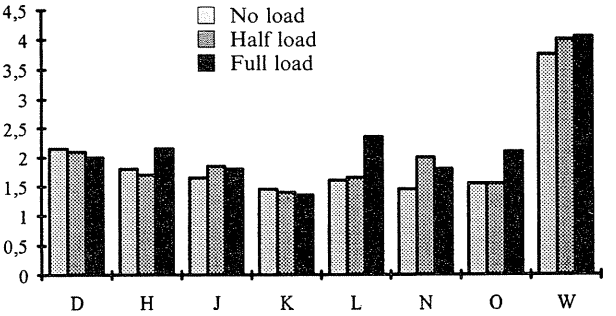

Fig. 41. The histogram of the settling time in real time application.

the various loads is achieved by the controller K. The other controllers may be sorted as follows: O, N, J, L, H, D and W.

Table 13 shows the disturbance rejection times obtained on the real platform for different loads. The histogram of this specification is illustrated in Fig. 42. The minimum disturbance rejection time for various loads is achieved by the controllers N and O. The other controllers may be sorted as follows: L, K, H, D, J and W.

Since the frequency characteristics of the designs cannot be examined in real time, the designs may only be compared in the time domain. The rise time, settling time and the disturbance rejection time are the major time characteristics of the system (the overshoot condition is satisfied by all of the designs so it is not considered). The sum of the normalised rise time, settling time and disturbance rejection time may be considered as a performance index for evaluating the different designs in real time application. The rise time and rejection of disturbance time are normalised by 1 s and 1.2 s, respectively, and the settling time is normalised by the average of the smallest values obtained in real time for the three different loadings (1.4 s). The results obtained are shown in Fig. 43 and in Table 14. To a large extent the real time experiments confirm the simulation results. The design N gives the best results but it is twice as com-

Table 13. The disturbance rejection time (s) in real time application.

	No load	Half load	Full load
D	1.90	1.25	2.10
H	1.55	1.20	1.65
J	2.10	1.70	1.60
K	1.60	1.15	1.40
L	1.45	1.10	1.40
N	1.35	1.00	1.50
O	1.10	1.30	1.45
W	2.25	2.00	2.95

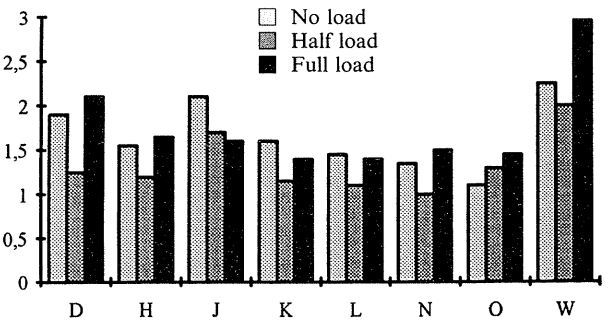

Fig. 42. The histogram of the disturbance rejection in real time application.

Table 14. The normalised sum of the rise times, settling times and disturbance rejection times in different loadings and for various designs.

N	K	O	L	J	H	D	W
9.47	9.65	10.72	10.86	11.47	11.50	12.70	22.63

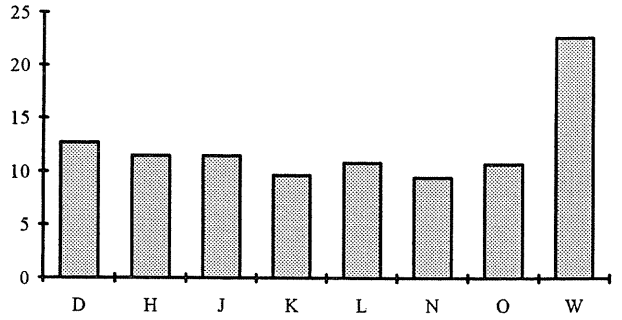

Fig. 43. The histogram of the normalised sum of the time characteristics in real time application.

Table 15. The joint performance / complexity criterion in real time application.

K	N	L	O	H	D	J	W
10.55	11.47	12.06	12.12	12.4	14.4	14.97	24.13

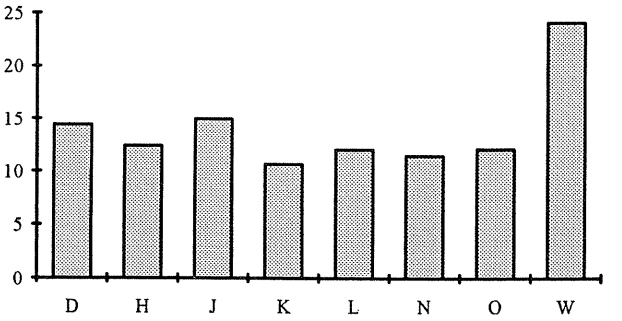

Fig. 44. The histogram of the joint performance / complexity criterion.

plex as the design K which gives extremely close performances. The designs O, L and H give also good results with a reasonable complexity. The design J gives good results but has the largest complexity.

One can attempt to define a single criterion in order to capture both performance and complexity by adding to the previous global performance criterion a normalised penalty term defined as: number of controller parameters divided by 10. Although this choice can be challenged, it may give a good image of the trade off: performance versus complexity. The results are summarised in Table 15 and illustrated in Fig. 44.

7. Conclusions

A flexible transmission system as a benchmark problem for robust digital control has been presented. Despite very large variations of the vibration modes with the load, a robust digital controller with acceptable performances can be designed using a variety of methods. The simulation results of eight different solutions to this benchmark have been analysed.

The performance satisfaction of the designs and their complexity have been evaluated. All of the specifications have been satisfied in simulation by one of the controllers (the controller N [10]) but with the price of a much higher complexity compared to the other controllers providing close performances. The controllers O [12], K [9], H [6] and L [11] give results which are close to that of the controller N but have less complexity. The controller W [8] is very far from the specifications. The controller J [7] despite reasonable performances has the largest complexity.

The experimental results have confirmed to a large extent the simulation results. The best time performance on the real plant has also been achieved by the controller N. In our opinion the controller K gives the best compromise performance/complexity followed closely by N, L, O and H.

The solution of Pan and Furuta [14] was not considered in the comparison because it is not a linear controller. However a comparison of the simulation results in time domain shows that its performances are lower than those of almost all of the other linear controllers.

It may be concluded that almost all of the design approaches are able to solve the problem. The QFT approach seems to be the best suited for this benchmark while H_∞ optimisation seems to be least suited for this benchmark. Further insight for the use of the approach to this problem can be found in [15].

The discrepancy in the complexity of the controllers (even for the case when the same theoretical approach is used by two designers) shows in our opinion that much work has to be done in order to develop a systematic methodology for designing robust digital controllers based on identified discrete time models, which will also take into account the complexity.

The design time seems to be an interesting criterion for evaluating the various designs, but, unfortunately, no information about this was available.

References

1. M'Saad M, Duque M, Hammad S. Flexible mechanical structures adaptive control. Adaptive Control Strategies for Industrial Use. C. Shah and G. Dumont (eds.), Springer, Berlin, 1989
2. M'Saad M, Hejda I. Adaptive control of a flexible transmission system. Control Engineering Practice, 1984; 2: 629–639
3. Adaptech PIM/TR, PC-REG, PC-REG/TR Users' manuals, Version 5, 1993, 4 rue du Tour de l'Eau, St-Martin d'Hères, France
4. Landau ID. System Identification and Control Design. Prentice Hall, Englewood Cliffs, NJ, 1990
5. Decker C, Ehrlinger AU, Boucher P, Dumur D. Application of constrained receding horizon predictive control to a benchmark problem. European J Control 1995; 1:157–165
6. Hjalmarsson H, Gunnarsson S, Gevers M. Model free tuning of a robust regulator for a flexible transmission system. European J Control 1995; 1:148–156
7. Jones NW, Limebeer DJN. A digital H_∞ controller for a flexible transmission system. European J Control 1995; 1:134–140
8. Walker DJ. Control of a flexible transmission—a discrete time H_∞ loop shaping approach. European J Control 1995; 1:141–147
9. Kidron O, Yaniv O. Robust control of uncertain resonant systems. European J Control 1995; 1:104-112
10. Nordin M, Gutman PO. Digital QFT design for the benchmark problem. European J Control 1995; 1:97–103
11. Landau ID, Karimi A,Voda A, Rey D. Robust digital control of flexible transmissions using the combined pole placement/sensitivity function shaping method. European J Control 1995; 1:122–133
12. Oustaloup A, Mathieu B, Lanusse P. The CRONE control of resonant plants: application to a flexible transmission. European J Control 1995; 1:113–121
13. Landau ID. Adaptive control with a French touch. Plenary Lecture, ACC 1995, Seattle, USA.
14. Pan Y, Furuta K. VSS approach to the design of robust digital controller. European J Control 1995; 1:166–173
15. Kwakermaak H. Symmetries in Control System Design. In: Isideri A. (ed), Trends in Control. A European Perspective, Springer Verlag, London, 1995